

## RESEARCH REPORT

**First morpho-functional characterization of *Anemonia viridis* amoebocytes: a light microscopy study****J Fabrello\*, M Ciscato, D Asnicar, MG Marin, V Matozzo***Department of Biology, University of Padova, Via Bassi 58/B, 35131, Padova, Italy**This is an open access article published under the CC BY license**Accepted December 6, 2022***Abstract**

For the first time, we studied the morpho-functional characteristics of amoebocytes of the sea anemone *Anemonia viridis*. A histochemical approach was adopted and two subpopulations of amoebocytes from mesoglea were observed: granulocytes and hyalinocytes. Granulocytes showed a high number of cytoplasmic granules, while hyalinocytes had no or few granules. Amoebocytes showed both round and spreading shapes and were divided in basophil, neutrophil or acidophil cells. Amoebocytes actively phagocytized yeast cells and produced superoxide anion. The presence of hydrolytic enzymes in amoebocytes was also investigated. Positive cells to acid phosphatase, acid esterase and non-specific esterase were found, with granulocytes and hyalinocytes that did not show different responses in term of positivity. Although preliminary, the results of this study can help to understand the features and immune role of *A. viridis* amoebocytes and the development of defense strategies in multicellular organisms. Moreover, this study lay the foundations for future more in-depth studies, including those at the ultrastructural level.

**Key Words:** amoebocytes; sea anemones; anthozoans; *Anemonia viridis*; hydrolytic enzymes**Introduction**

Anthozoans are the largest cnidarian group and are widely distributed in marine environments. Beside of 7200 anthozoans species are known, these animals are poorly studied (Kayal *et al.*, 2018). However, the features of their immune system and their biochemical effectors have recently been investigated. The first defense barrier, in these animals, is the mucus layer, that is a polysaccharide protein lipid complex covering the animal's body (Mydlarz *et al.*, 2016). Other passive immune defense systems are the antimicrobial secondary metabolites and antimicrobial peptides that are typically cationic membrane bound peptides and have bactericidal activity (Mydlarz *et al.*, 2016). Furthermore, the presence of pattern recognition receptors (PRRs) has been demonstrated in anthozoans, indeed both toll-like receptors (TLRs) and nod-like receptors (NLRs), two of the main PRR classes, have been detected (Orús-Alcalde *et al.*, 2021; Guryanova and Ovchinnikova, 2022).

However, organisms have also cellular effectors, called amoebocytes. These cells can move through

the tissues and can aggregate near wound sites reacting also to grafts (Patterson and Landolt, 1979; Meszaros and Bigger, 1999; Mydlarz *et al.*, 2008; Couch *et al.*, 2013). Amoebocytes can perform phagocytosis (Watson and Mariscal, 1983; Larkman, 1984). Indeed, it has been demonstrated that these cells react against bacterial and fungal infections and move to the injured areas (Meszaros and Bigger, 1999; Mydlarz *et al.*, 2008; Hutton and Smith, 1996). For instance, an increased number of elongated amoebocytes with irregularly round nuclei was observed in the mesoglea near the new epidermal layer in *Anemonia viridis* specimens after tentacle amputation (Parisi *et al.*, 2021). The authors also observed collagen fibrils surround the elongated amoebocytes suggesting their fibroblastic nature (Parisi *et al.*, 2021). Moreover, in gorgonians, trauma induced the activation of phagocytic cells such as granular amoebocytes and the phagocytosis in cells not usually phagocytic cells (Olano and Bigger, 2000). Similarly, in the sea anemone *Metridium senile* during regeneration, amoebocytes actively phagocytized (Polteva, 1970). Interestingly, thermal injury caused the immigration of phagocytes that eliminated necrotic tissue and promoted repair in the anthozoan *Anthopleura elegantissima* (Patterson and Landolt, 1979).

Amoebocytes have been observed within the mesoglea of anthozoans (Patterson and Landolt, 1979; Hutton and Smith, 1996; Parisi *et al.*, 2021).

*Corresponding author:*

Jacopo Fabrello  
Department of Biology  
University of Padova  
Via Bassi 58/B, 35131, Padova, Italy  
E-mail: jacopofabrello@gmail.com

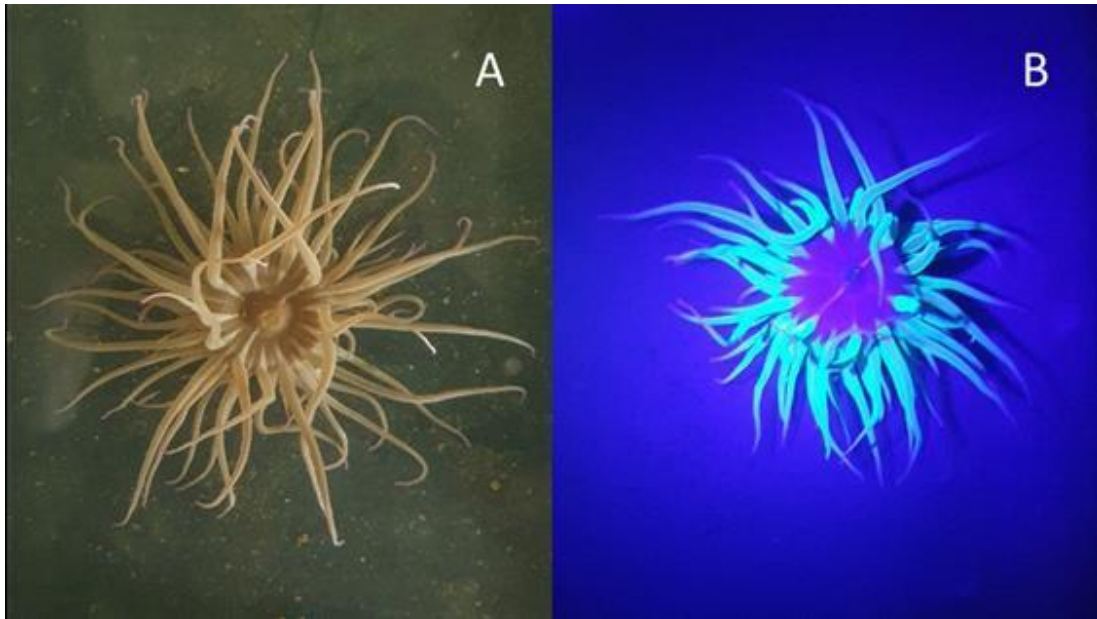


**Fig. 1** *A. viridis* (variety *viridis*) specimens under natural light (A) and detectable after irradiation with ultraviolet light (395 nm) (B)

For instance, amoebocytes were observed in the mesoglea of the sea anemone *Nematostella vectensis* and in *Anemonia sulcata* (Tucker *et al.*, 2011; Gadelha *et al.*, 2013). Similarly, in *Anemonia fragacea*, amoebocytes were commonly observed among the epithelial cell base near mesoglea, showing mainly a round shape. While in the mesoglea, amoebocytes showed more variable forms and were highly irregular and fusiform near the mesenteric retractor muscle (Larkman, 1984). Two main amoebocytes types have been observed: granulocytes and hyalinocytes (Mullen *et al.*, 2004; Reed *et al.*, 2010; Tucker *et al.*, 2011). Amoebocytes with granules, also named granulocytes, were observed in several cnidarians (Mydlarz *et al.*, 2008; Watson and Mariscal, 1983; Parisi *et al.*, 2014). For instance, granular amoebocytes have been noted in *Actinia fragacea* often showing an irregular shape with numerous cytoplasmic granules (Larkman, 1984). These granules were usually spherical or slightly elongated (mean diameter of 300 nm) and did not contain homogeneous materials (Larkman, 1984). Granulocytes have been observed near fungal infection areas (Mydlarz *et al.*, 2008). The same authors documented melanosomes in granular amoebocytes near the infection area in *Gorgonia ventalina*, suggesting that some amoebocytes subpopulations can participate in the melanin synthesis pathway (Mydlarz *et al.*, 2008). Interestingly, granular amoebocytes react not only against biotic stressors, but also against abiotic ones. Indeed, amoebocytes increased in soft coral *G. ventalina* specimens exposed to increasing water temperature over 8 days (Mydlarz *et al.*, 2008). In an opposite way, hyalinocytes have numerous small, non-refractile granules (Hutton and Smith,

1996). These cells phagocytized the gram-negative bacterium *Psychrobacter* in *Actinia equina* (Hutton and Smith, 1996), while in *A. viridis*, hyalinocytes acted as fibroblast-like cells, synthesizing collagen (Parisi *et al.*, 2021).

*A. viridis* is a common Mediterranean anthozoans, from the Portugal coast up to Irish Atlantic Ocean. It is a benthic organism that inhabit rocks and as the other anthozoans can only slowly move away from a non-optimal environment. This means that they are subjected to physic-chemical environmental alterations, and they cannot rapidly move away. As many other anthozoans this animal lives in symbiosis with zooxanthella. This microalgae of genus *Symbiodinium* provide energy to the animals thanks to the photosynthesis. For this reason, the self and non-self recognition is very important in these animals. However, many aspects of amoebocytes, including the enzymes used to destroy non-self materials, are still unknown. The aim of this study was to define for the first time morpho-functional characteristic of amoebocytes in *A. viridis*.

## Materials and Methods

### Animal collection

A total of fifteen *A. viridis* (variety *viridis*) (Fig. 1A-1B) specimens were sampled by hand in the Lagoon of Venice, near Chioggia (mean diameter 7.3 cm). Animals were maintained for 7 days before analyses in large aquaria with aerated seawater (salinity of  $35 \pm 1$ ; temperature  $16 \pm 0.5$  °C) that was renewed every two days. At the same time animals were fed with pieces of mussels (*Mytilus galloprovincialis*). Analyses were performed in triplicate.

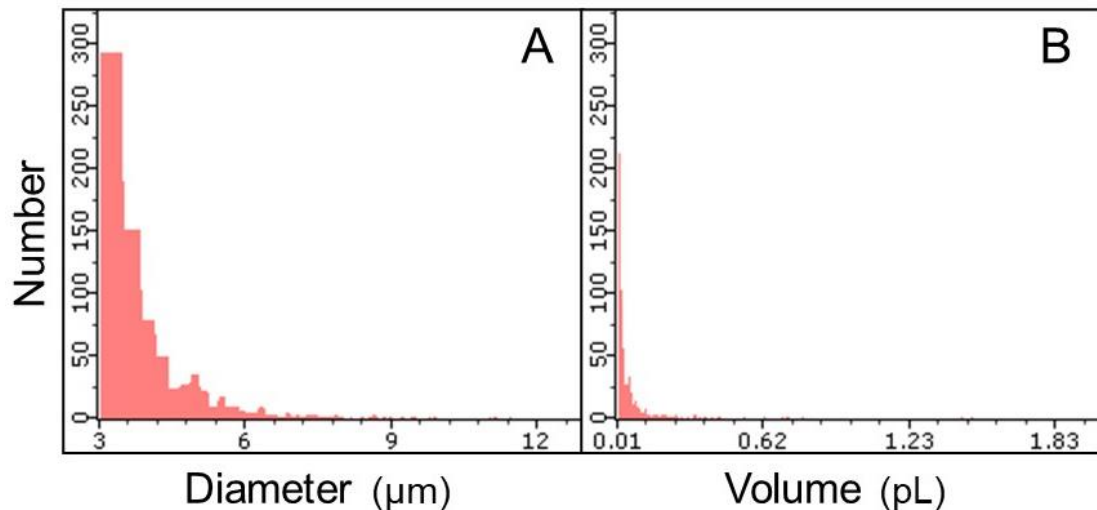


**Fig. 2** An example of amoebocyte size frequency distribution in *A. viridis*. Amoebocyte diameter (A), expressed in  $\mu\text{m}$ , and amoebocyte volume (B), expressed in picolitres (pL)

#### Cell sampling

Mesoglea cells were withdrawn with a syringe from tentacles and the pedal disc of three animals. Except for cell size and their frequency distribution analysis, samples were pooled on ice in a test tube by adding 0.38% sodium citrate in 0.45  $\mu\text{m}$  of filtered seawater (FSW), pH 7.5, in the proportion of 1:15 to prevent clotting.

#### Amoebocytes size

Total cell count and amoebocytes size were evaluated using a Scepter™ 2.0 Automated Cell Counter (Millipore, FL, USA). Analyses were performed in triplicate and no anti-clotting or fixative were added to the pooled samples. Diameter and volume were expressed in  $\mu\text{m}$  and picolitres respectively.

#### Cytochemical assays

After amoebocyte collection, samples were centrifuged at 800 g for 10 minutes and cells were carefully resuspended in a reduced volume of FSW to concentrate them. To perform cytochemical assays we used culture chamber made with glued Teflon rings (15 mm internal diameter, 1 mm thickness) on glass slides as developed by Ballarin *et al.* (1994). Briefly, 60  $\mu\text{L}$  of sample were kept in the chamber that was then covered with a coverslip adding some vaseline on the ring to allow its adhesion. After, culture chambers were kept upside down at room temperature for 30 minutes to allow the cell adhesion to the coverslips. Then, cells were fixed for 30 min at 4 °C in glutaraldehyde 1% in FSW with 1% of sucrose, washed in phosphate buffer saline (PBS) 0.01 M and stained as follows:

- *Giemsa's staining*: after fixation cells were stained for 7 min using Giemsa 5% in FSW, washed in distilled water and mounted on a glass slide using Aquovitrex (Carlo Erba, Milan).

- *Ehrlich's triacid mixture*: the mixture is composed of 12 parts of saturated Orange G aqueous solution, 8 parts of saturated acid fuchsin aqueous solution, 10 parts of saturated methyl green aqueous solution, 30 parts of distilled water, 18 parts of absolute ethanol and 5 parts of glycerin. Cells were stained in this mixture for 15 min, washed in distilled water and mounted. Basophilic granules appeared pale green, neutrophilic violet and acidophilic coppery red.

- *Sudan black B staining*: after fixation, cells were washed in PBS and treated for 3 min with 50% ethanol and immersed for 15 min in a saturated solution of Sudan Black B in 70% ethanol. Slides were then immersed in 50% ethanol, washed with distilled water and mounted. Black spot revealed the presence of lipids.

- *Phagocytosis*: after the adhesion, cells were incubated for 1 h with a yeast solution (*Saccharomyces cerevisiae*; 1:10 cells/yeast ratio) at room temperature in culture chambers (Cima *et al.*, 2000). After that, slides were washed several times with FSW and then fixed. Subsequently, slides were washed for 10 min in PBS, stained for 7 min using Giemsa 5% and mounted. Phagocytosing cells were observed under light microscope.

- *Intracellular superoxide anion*: intracellular  $\text{O}_2^-$  was detected following the method of Song and Hsieh (1994), both in the presence or absence of yeast. In detail, after the incubation in yeast or directly using no exposed cells, amoebocytes were incubated for 60 min with 0.2% nitro blue tetrazolium (NBT) in FSW, fixed as described above and washed for 10 min in PBS. The reaction product (formazan) was solubilized by adding a solution containing 120  $\mu\text{L}$  of 2 M KOH and 140  $\mu\text{L}$  of DMSO for 30 min. The slides were then mounted using Aquovitrex. The granules of precipitated formazan appeared in blue.

- *Acid phosphatase*: Fixed amoebocytes were washed for 10 min in 0.1 M sodium acetate buffer, pH 5.2, and then incubated for 1 h at 37 °C in a mixture, as reported by Lojda (1962). The mixture contained 10 mg naphthol AS-BI phosphate (Sigma) dissolved in 400 µL dimethylformamide (DMF), 400 µL solution A (0.4 g pararosaniline (Fluka), 2 mL HCl 37%, 8 mL distilled water), 400 µL solution B (4% NaNO<sub>2</sub> in distilled water) and 20 mL of 0.1 M sodium acetate buffer (pH 5.2). Positive cells were stained red.

- *Non-specific esterase*: the method of Gomori (1948) was used. Fixed cells were washed 10 min in PBS and then incubated for 3 h at 4 °C in mixture. The mixture was made dissolving 0.01 g naphthol AS-D acetate in 1 mL acetone and adding 0.08 g Fast-Blue dye previously dissolved in 50 ml with PBS. After incubation, slides were washed for 10 min in PBS and mounted. Positive cells were stained black.

- *Acid esterase*: the presence of acid esterase was detected following the method of Lojda (1977). In detail, fixed cells were washed 10 min in citric acid phosphate buffer (0.1 M, pH 5.5)

and then incubated for 16 h at 4 °C in a mixture. The mixture contained 3 mg naphthol AS-D acetate dissolved in 500 µL acetone, 125 µL solution A, 125 µL solution B and 20 mL of citric acid phosphate buffer. After incubation, slides were washed with distilled water and mounted. Positive cells were stained pink-brown.

In each assay, cells were observed under light microscope (LM) at 1000x and analyzed using Leica image software LAS ver. 4.12.0, Leica Microsystems.

### Results

A mean cell concentration of  $2.2 \times 10^6$  cell/mL was detected, with a mean cell diameter and volume of 4.44 µm and 0.045 pL, respectively (Fig. 2A-B). Under LM, two main cell types were observed: granulocytes with many cytoplasmatic granules (Fig. 3A) and hyalinocytes that show a homogeneous cytoplasm with no or few granules (Fig. 3B). The common cell shape was round, but we also observed some spreading cells (Fig. 3C, 3D).

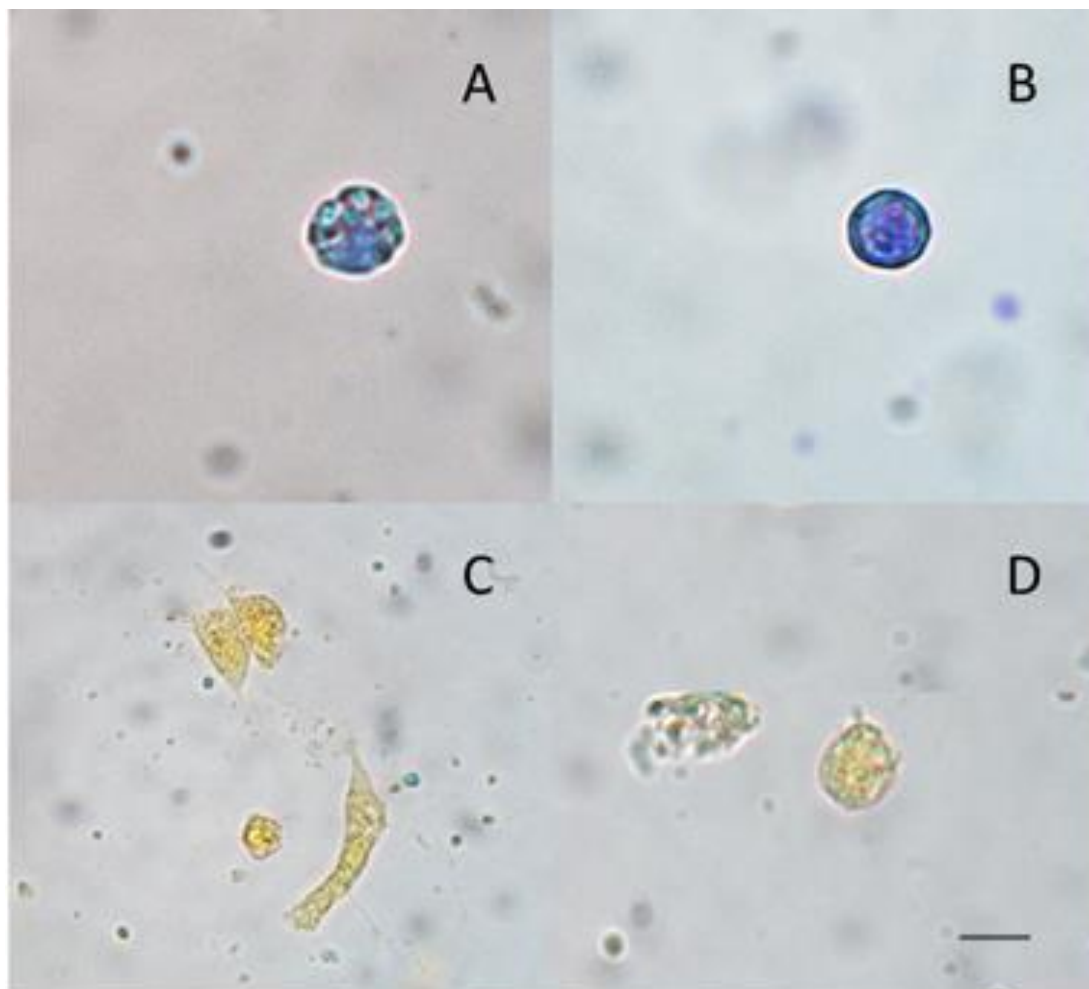


**Fig. 3** Micrographs of *A. viridis* amoebocytes stained with Giemsa's dye: granulocyte (A), hyalinocyte (B). Spreading amoebocytes (C), round amoebocyte (D). Bar length: 5 µm

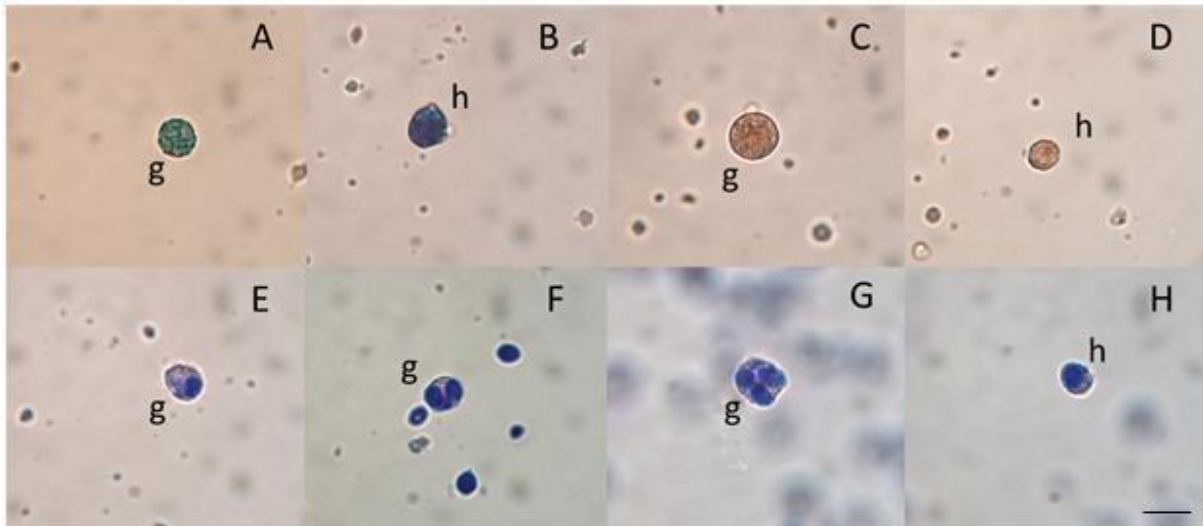


**Fig. 4** *A. viridis* amoebocytes stained with Ehrlich's triacid mixture (A, B, C, D). Basophil granulocyte (A), neutrophil hyalinocyte (B), acidophil granulocyte (C), acidophil hyalinocyte (D). Amoebocytes phagocytizing yeast cells (E, F, G, H). Granulocyte (E, F, G) and hyalinocyte (H) with engulfed yeast cells; g: granulocyte; h: hyalinocyte. Bar length: 5  $\mu$ m

Ehrlich's staining highlighted cells with basophil (Fig. 4A), neutrophil (Fig. 4B) and both acidophil granules and acidophilic cytoplasm (Fig. 4C, 4D). Both granulocytes and hyalinocytes phagocytized yeast cells (Fig. 4E-H), in which up to three yeast cells were engulfed (4G).

Interestingly, both granulocytes and hyalinocytes appeared positive to acid phosphatase activity (Fig. 5A-C), non-specific esterases (Fig. 5D-F) and acid esterase (Fig. 5G-I).

Furthermore, all cell types showed black deposits after Sudan black staining, indicating lipids, mostly on cell membranes (Fig. 5J-K-L).

Lastly, we evaluated superoxide intracellular anion production without stimulation of yeast cells (phagocytosis). Interestingly, no deposit of blue deposits of formazan were observed (Fig. 6A-B). However, after incubation with yeast, superoxide anion production was revealed (Fig. 6C-D). We did not observe a different response in terms of production of formazan blue deposits between granulocytes and hyalinocytes.

A summary of amoebocytes properties is reported in Table 1.

## Discussion

We analyzed for the first time the morpho-functional characteristic of amoebocytes of *A. viridis*. The mean diameter of amoebocytes (4.4  $\mu$ m) in *A. viridis* was smaller than that of phagocytes found in the two hexacorals *Pocillopora damicornis* and *N. vectensis*, 10-20  $\mu$ m and 10-15  $\mu$ m respectively (Snyder *et al.*, 2021). Moreover, in the gorgonian *Plexaurella fusifera*, amoebocytes near wound had a size ranged from 5-9  $\mu$ m in width and from 8 to 15  $\mu$ m in length, with a nuclear mean diameter of 3.5-4  $\mu$ m (Meszaros and Bigger, 1999),

like to what was observed in *A. fragacea* amoebocytes (Larkman, 1984). We observed amoebocytes with both round and amoeboid shape. Interestingly, Hutton and Smith (1996) reported that most spreading cells were hyaline cells, but spreading shape was largely dependent upon the presence of coelenteron fluid. Our resuspension in FSW could explain why we observed a slow amount of spreading cells, however Hutton and Smith (1996) used a different model species (*A. equina*).

We observed two types of amoebocytes within the mesoglea: granulocytes and hyalinocytes. Granulocytes showed a high number of cytoplasmic granules. In some cells, granules were few and big, while in other cells there was a high number of small granules. On the contrary, hyalinocytes either had no granules or very few. These observations agree with the results of Hutton and Smith (1996). Indeed, in *A. equina*, they observed two distinct cell types: hyaline cells, that contained numerous small granules, and granular cells, that contained large granules with a usual proportion of 5:1. In *A. equina*, Parisi *et al.* (2014) reported six cell types from percolated animal body fluid: morular granulocytes, cells with large or small peripheral granules, granulocytes (with irregular shape containing blue and red granules), cells showing one fine red granule of uniform size and, finally, cells with elongated shape and small dispersed granules. Moreover, they observed that granulocytes can cause plaque of lysis versus mammals' erythrocytes (Parisi *et al.*, 2014). In addition, in the octocoral *Swiftia exserta* two types of immunocytes have been observed: "oblong granular cells" and "granular amoebocytes." These two subpopulations differed for both the enzyme reactivity and their location within the mesoglea (Menzel and Bigger, 2015).

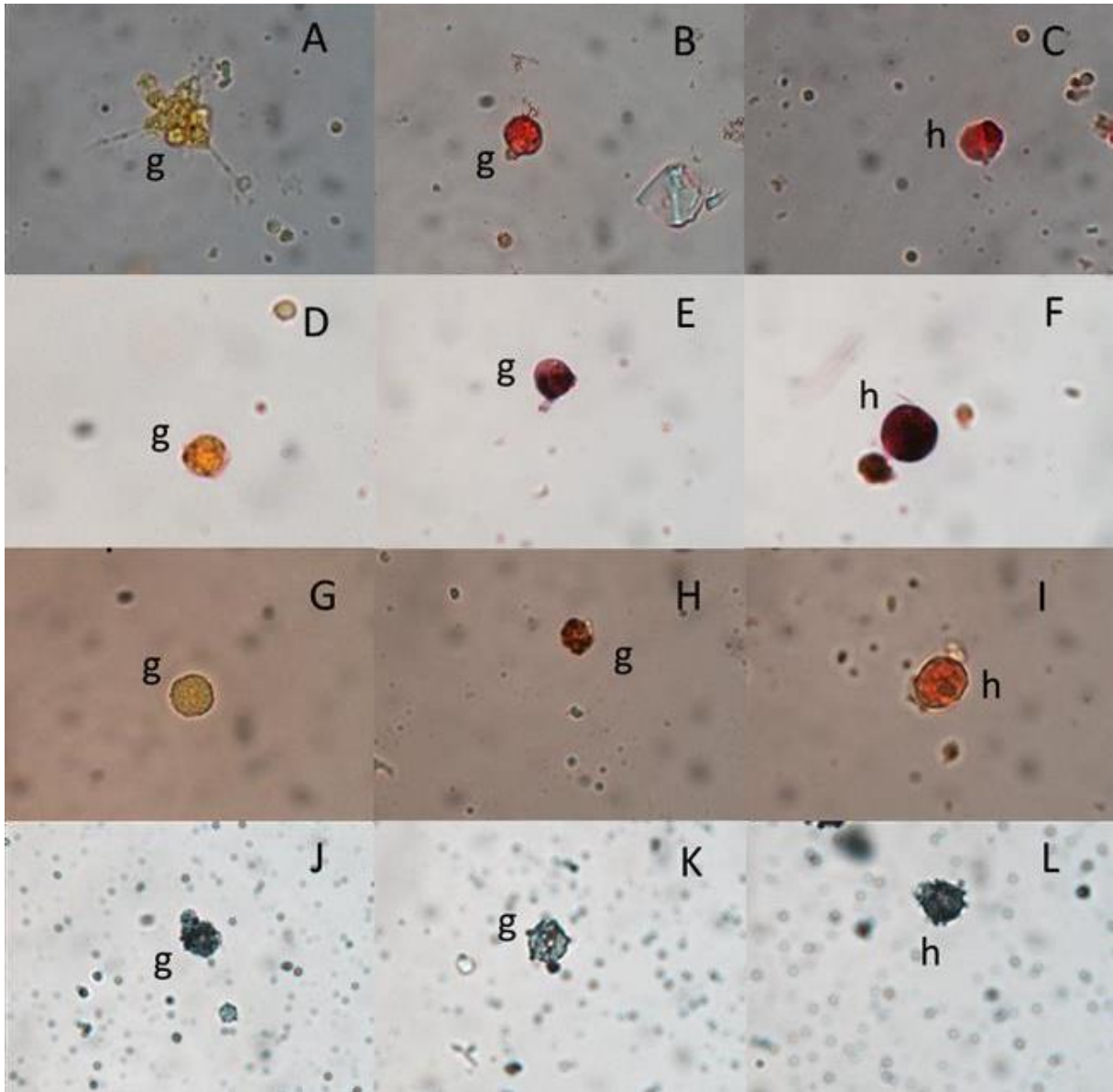


**Fig. 5** Light micrographs of *A. viridis* amoebocytes. Acid phosphatase (A, B, C): negative granulocyte (A), positive granulocyte (B), positive hyalinocyte (C). Non-specific esterase (D, E, F): negative granulocyte (D), positive granulocyte (E), positive hyalinocyte (F). Acid esterase (G, H, I): negative granulocyte (G), positive granulocyte (H), positive hyalinocyte (I). Sudan black B (J, K, L): positive granulocyte (J), positive granulocyte (K), positive hyalinocyte (L); g: granulocyte; h: hyalinocyte. Bar length: 5  $\mu$ m

We demonstrated that amoebocytes can engulf yeast cells. Phagocytosis appears to be performed by several cell types in cnidarians, as reported in the gorgonian *S. exserta*, in which granular amoebocytes, epidermal cells, sclerocytes, mesogleal cells, and gastrodermal cells were active phagocytes against foreign particles (Olano and Bigger, 2000). In addition, in *A. equina*, hyaline amoebocytes were the only subpopulation showing phagocytic activity *in vitro* against the gram-negative bacterium *Psychrobacter immobilis* (Hutton and Smith, 1996). It has been demonstrated that amoebocytes participate in the wound healing. This

process was studied in deep in *Porites cylindrica* and in *Acropora millepora*, in which plug formation via degranulation of melanin-containing granular cells occurs. Then as inflammatory response, the eosinophilic granular amoebocytes infiltrate the area and fibroblast and agranular hyaline cells help to connect the tissue. Lastly there is the granular tissue formation, its differentiation and the remelanization of eosinophilic granular amoebocytes (Mydlarz *et al.*, 2016).

The Erlich's triacid staining revealed the presence of basophil, neutrophil, and acidophil cells in *A. viridis*. Amoebocytes with acidophilic granules

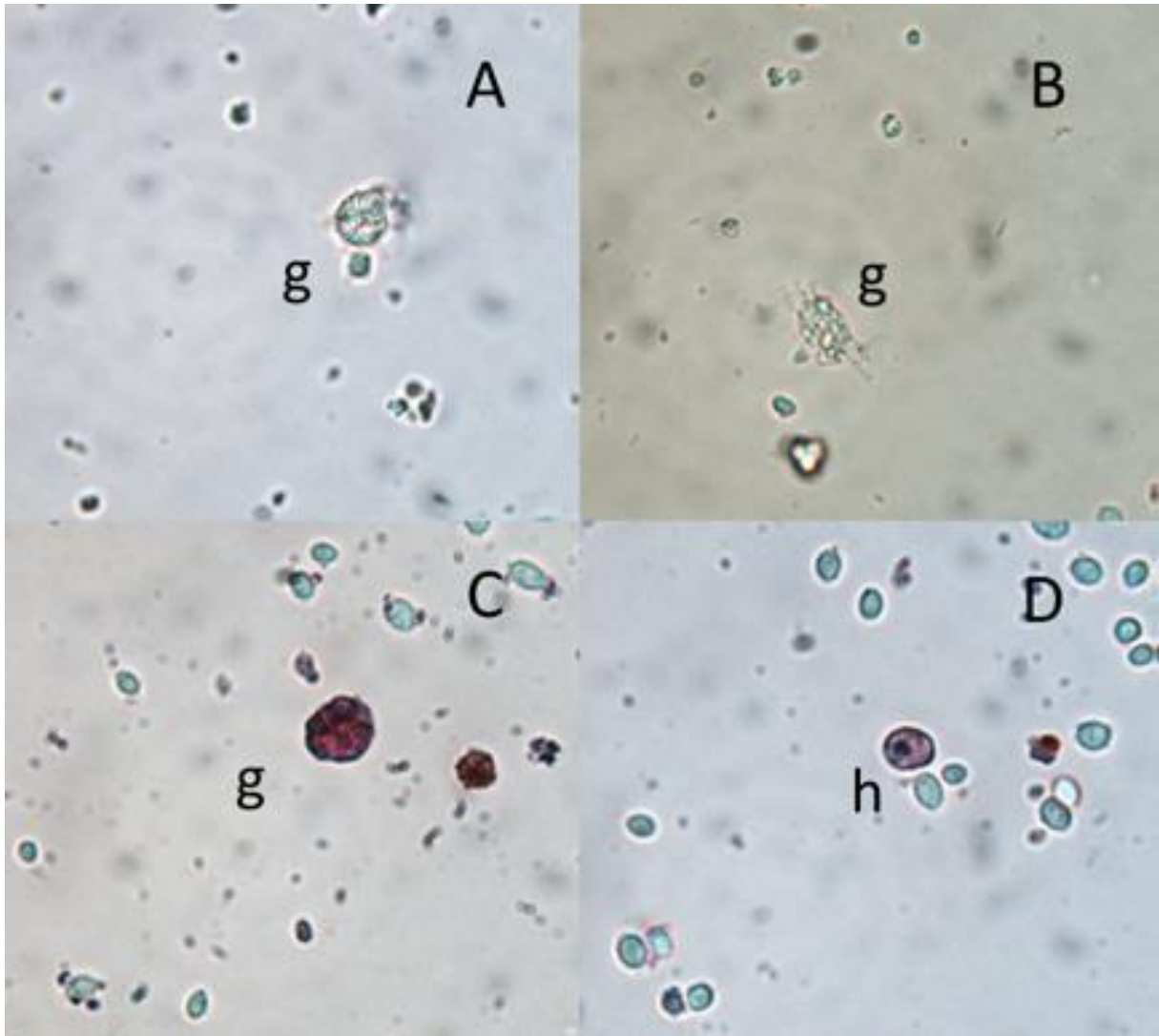


**Fig. 6** Intracellular superoxide anion detection (A-D): negative granulocytes (A, B), positive granulocyte (C), positive hyalinocyte (D)

have been observed in the scleractinian coral *Montastraea cavernosa* (Vargas-Ángel *et al.*, 2007), in which also a coalescence of granular amoebocytes during tissue repair was noted (Renegar, 2015). In addition, amoebocytes of *P. fusifera* located near wound showed granules (0.5 to 1.5  $\mu\text{m}$  in diameter) that were mostly eosinophilic. However, some amoebocytes showed slightly basophilic granules (Meszaros and Bigger, 1999). Similar results were obtained in the hard coral *P. cylindrica* in which a dense eosinophilic granular amoebocytes aggregation was observed after injury (Palmer *et al.*, 2011). The same authors observed round agranular cells, melanin-containing granular cells and fibroblasts (Palmer *et al.*, 2011). While using ematossil-eosin staining, Patterson and Landolt (1979) observed neutrophils and eosinophils granules in amoebocytes.

In *A. viridis*, lipids were observed on cell membrane and in cytoplasm of amoebocytes as

black spots produced after Sudan Black B staining. In agreement, Larkman (1984) indicated that granular amoebocytes in *A. fragacea* – distributed in both mesoglea and epithelial cell layers – contained extensive glycogen deposit and lipid droplets. Moreover, in granulocytes of gorgonian *Pseudoplexaura flagellosa* specimens infected with a green filamentous alga, granules positive for Periodic Acid Schiff (PAS) reaction were observed (Colley, 1987). Similarly, amoebocytes of the soft coral *P. fusifera* located near wound appeared positive to PAS reaction (Meszaros and Bigger, 1999).

In this study, we investigated the presence of some hydrolytic enzymes in amoebocytes of *A. viridis*. We observed that cells were positive to acid phosphatase, acid esterase and non-specific esterase assays, hydrolytic enzymes that can play with an important immune role. Similarly, Watson and Mariscal (1983), reported that granules of

**Table 1** Cytochemical properties of *A. viridis* amoebocytes. +: positive; -: negative

	Granulocytes	Hyalinocytes
Giemsa's dye	+	+
Ehrlich's triacid mixture	+	+
Sudan black B dye	+	+
Phagocytosis	+	+
Intracellular O <sub>2</sub> <sup>-</sup>	-	-
Intracellular O <sub>2</sub> <sup>-</sup> with yeast	+	+
Acid phosphatase	+	+
Non-specific esterase	+	+
Acid esterase	+	+

amoebocytes were positive for the acid phosphatase in the tentacles of the sea anemone *Haliplanella luciae*, concluding that these dense granules were primary lysosomes. Furthermore, Menzel and Bigger (2015) performed several cytochemical assays on coenenchyma cells of the octocoral *S. exserta*. They found that oblong cells with large granules in the mesogleal cell cords were quinone-reactive cells with high concentrations of quinones and quinoproteins. Interestingly cells were negative to both  $\beta$ -glucuronidase and alkaline phosphatase assays, but oblong granular cell were positive for acid phosphatase assay. On the contrary, granules of the amoebocytes from *A. fragacea* were feebly positive to the acid phosphatase assay, while the matrix of residual body-like inclusions observed in amoebocytes showed acid phosphatase activity suggesting a lysosomal nature (Larkman, 1984). The suggestion that amoebocytes have anti-bacterial activities was also reported by Hutton and Smith (1996): they observed that the amoebocyte lysate contain soluble bactericidal factors that probably were not lysozyme-like enzymes. Menzel and Bigger (2015) observed that oblong granular cells, granular amoebocytes and also morula-like cells of the coral *S. exserta* were positive to acetate esterase assay. In addition, in *A. sulcata* Trapani *et al.* (2016) observed an increase of both alkaline phosphatase and esterase activity in both the body and tentacles of specimens injected with bacteria.

In the present study, superoxide anion production was revealed only after incubation of amoebocytes with yeast cells. It has been demonstrated that amoebocytes of *A. equina* produced superoxide anion after stimulation with phorbol myristate acetate or lipopolysaccharide (Hutton and Smith, 1996). Lastly, a low pH in lysosomal vesicles and an increase in ROS activity was observed during phagocytosis in two hexacorallians (Snyder *et al.*, 2021).

## Conclusion

Based on morphological features, we can state that two amoebocyte types circulate in *A. viridis*. These cells have presumably an important immunity role, phagocytizing foreign material and destroying non-self materials with hydrolytic enzymes and superoxide anion. Interestingly, the two amoebocyte populations did not show differences in term of positivity to enzymatic activity assays. However, the relationship between granulocytes and hyalinocytes still remain unknown. Although preliminary, results of this study can help to understand the features of *A. viridis* amoebocytes and their involvement in immune responses. However, further investigations are needed, including those at the ultrastructural level.

## References

- Ballarin L, Cima F, Sabbadin A. Phagocytosis in the colonial ascidian *Botryllus schlosseri*. *Dev. Comp. Immunol.* 18: 467-481, 1994.
- Cima F, Matozzo V, Marin MG, Ballarin L. Haemocytes of the clam *Tapes philippinarum* (Adams & Reeve, 1850): morphofunctional characterization. *Fish Shellfish Immunol.* 10: 677-693, 2000.
- Colley SB. A histochemical and electron microscopical study of a gorgonian coral infected with a green filamentous alga. Master thesis, Florida Atlantic University, Boca Raton, Florida, 1987.
- Couch CS, Weil E, Harvell CD. Temporal dynamics and plasticity in the cellular immune response of the sea fan coral, *Gorgonia ventalina*. *Mar. Biol.* 160: 2449-2460, 2013.
- Gadelha JR, Morgado F, Soares AMVM. Histology and histochemistry of sea anemones in environmental contamination studies. *Microsc. Microanal.* 19: 57-58, 2013.
- Gomori G. Histochemical demonstration of sites of choline esterase activity. *Proc. Soc. Exp. Biol. Med.* 68: 354-358, 1948.

- Guryanova SV, Ovchinnikova, TV. Innate immunity mechanisms in marine multicellular organisms. *Mar. Drugs* 20: 549, 2022.
- Hutton DM, Smith VJ. Antibacterial properties of isolated amoebocytes from the sea anemone *Actinia equina*. *Biol. Bull.* 191: 441-451, 1996.
- Kayal E, Bentlage B, Pankey MS, Ohdera AH, Medina M, Plachetzki DC, *et al.* Phylogenomics provides a robust topology of the major cnidarian lineages and insights on the origins of key organismal traits. *BMC Evol. Biol.* 18: 1-18, 2018.
- Larkman AU. The fine structure of granular amoebocytes from the gonads of the sea anemone *Actinia fragacea* (Cnidaria: Anthozoa). *Protoplasma* 122: 203-221, 1984.
- Lojda Z. Detection of acid phosphatase. In *Proceedings of the 1st Conference of Czechoslovak Histochemical Committee*, 28 September 1962.
- Lojda Z. Studies on glycyl-proline naphthylamidase. *Histochemistry* 54: 299-309, 1977.
- Menzel LP, Bigger CH. Identification of unstimulated constitutive immunocytes, by enzyme histochemistry, in the coenenchyme of the octocoral *Swiftia exserta*. *Biol. Bull.* 229: 199-208, 2015.
- Meszaros A, Bigger C. Qualitative and quantitative study of wound healing processes in the coelenterate, *Plexaurella fusifera*: spatial, temporal, and environmental (light attenuation) influences. *J. Invertebr. Pathol.* 73: 321-331, 1999.
- Mullen KM, Peters EC, Harvell CD. Coral resistance to disease. In *Coral health and disease*, 1<sup>st</sup> ed.; Rosenberg E, Loya Y, Springer, Berlin, Heidelberg, 2004; Volume 1, pp. 377-399.
- Mydlarz LD, Fuess L, Mann W, Pinzón JH, Gochfeld DJ. Cnidarian immunity: from genomes to phenomes. In *The Cnidaria, Past, Present and Future*, 1<sup>st</sup> ed.; Goffredo S., Dubinsky Z.; Springer, Cham., Switzerland, Volume 1, pp. 441-466, 2016.
- Mydlarz LD, Holthouse SF, Peters EC, Harvell CD. Cellular responses in sea fan corals: granular amoebocytes react to pathogen and climate stressors. *PLoS One* 3: e1811, 2008.
- Olano CT, Bigger CH. Phagocytic activities of the gorgonian coral *Swiftia exserta*. *J. Invertebr. Pathol.* 76: 176-184, 2000.
- Orús-Alcalde A, Lu TM, Børve A, Hejnol A. The evolution of the metazoan Toll receptor family and its expression during protostome development. *BMC Ecol. Evo.* 21: 208, 2021.
- Palmer CV, Traylor-Knowles NG, Willis BL, Bythell JC. Corals use similar immune cells and wound-healing processes as those of higher organisms. *PLoS One* 6: e23992, 2011.
- Parisi MG, Grimaldi A, Baranzini N, La Corte C, Dara M, Parrinello D, *et al.* Mesoglea extracellular matrix reorganization during regenerative process in *Anemonia viridis* (Forskål, 1775). *Int. J. Mol. Sci.* 22: 5971, 2021.
- Parisi MG, Trapani MR, Cammarata M. Granulocytes of sea anemone *Actinia equina* (Linnaeus, 1758) body fluid contain and release cytolytic factors forming plaques of lysis. *Invertebr. Surviv. J.* 11: 39-46, 2014.
- Patterson MJ, Landolt ML. Cellular reaction to injury in the anthozoan *Anthopleura elegantissima*. *J. Invertebr. Pathol.* 33: 189-196, 1979.
- Polteva DG. Morphogenetic processes during somatic embryogenesis in *Metridium senile*. *Vestn. Leningr. Gos. Univ.* 9: 96-105, 1970.
- Reed KC, Muller EM, van Woesik R. Coral immunology and resistance to disease. *Dis. Aquat. Org.* 90: 85-92, 2010.
- Renegar DEA. Histology and Ultrastructure of *Montastraea cavernosa* and *Porites astreoides* During Regeneration and Recruitment: Anthropogenic Stressors and Transplant Success. Doctoral dissertation. Nova Southeastern University, Oceanographic Center, Florida, 2015.
- Snyder GA, Eliachar S, Connelly MT, Talice S, Hadad U, Gershoni-Yahalom O, *et al.* Functional characterization of hexacorallia phagocytic cells. *Front. Immunol.* 12: 662803, 2021.
- Song YL, Hsieh YT. Immunostimulation of tiger shrimp (*Penaeus monodon*) hemocytes for generation of microbicidal substances: analysis of reactive oxygen species. *Dev. Comp. Immunol.* 18: 201-209, 1994.
- Trapani MR, Parisi MG, Parrinello D, Sanfratello MA, Benenati G, Palla F, *et al.* Specific inflammatory response of *Anemonia sulcata* (Cnidaria) after bacterial injection causes tissue reaction and enzymatic activity alteration. *J. Invertebr. Pathol.* 135: 15-21, 2016.
- Tucker RP, Shibata B, Blankenship TN. Ultrastructure of the mesoglea of the sea anemone *Nematostella vectensis* (Edwardsiidae). *Invertebr. Biol.* 130: 11-24, 2011.
- Vargas-Ángel B, Peters EC, Kramarsky-Winter E, Gilliam DS, Dodge RE. Cellular reactions to sedimentation and temperature stress in the caribbean coral *Montastraea cavernosa*. *J. Invertebr. Pathol.* 95: 140-145, 2007.
- Watson GM, Mariscal RN. Comparative ultrastructure of catch tentacles and feeding tentacles in the sea anemone *Haliplanella*. *Tissue Cell.* 15: 939-953, 1983.